

High resolution, high collection efficiency in numerical aperture increasing lens microscopy of individual quantum dots

Zhiheng Liu and Bennett B. Goldberg

Department of Physics, Boston University, Boston, Massachusetts 02215

Stephen B. Ippolito, Anthony N. Vamivakas, and M. Selim Ünlü

Department of Electrical and Computer Engineering, Boston University, Boston, Massachusetts 02215

Richard Mirin

National Institute of Standards and Technology, Boulder, Colorado 80305

(Received 11 April 2005; accepted 28 June 2005; published online 9 August 2005)

We demonstrate the application of a subsurface solid immersion technique to the photoluminescence spectroscopy of individual quantum dots. Contrasted with the conventional solid immersion microscopy, we used a numerical aperture increasing lens and moved the interface between the sample and the solid immersion lens away from the focal plane, thus diminished the influence of interface artifacts on the images obtained in a two-dimensional scan. Meanwhile, our technique has achieved a high spatial resolution of $\lambda/3$ that is capable of resolving the spectroscopic features of single QDs. We also demonstrate that the collection efficiency of our system is six times better than that of a conventional confocal microscope with a high NA objective. © 2005 American Institute of Physics. [DOI: 10.1063/1.2012532]

Solid immersion microscopy (SIM)¹ has been a powerful tool to study optical properties of microstructures in recent years due to its high spatial resolution beyond diffraction limit,² as well as high efficiency of light collection.³ It is particularly suitable for the investigation of individual quantum dots (QD) whose dimensions lie in the scale of tens of nanometers.⁴ The deep sub-micron spatial resolution achieved by SIM⁵ ensured that only a few QDs are probed at a time so that inhomogeneous line broadening is eliminated. The improved light extraction from emitters⁶ enabled intensity-sensitive experiments such as time-resolved photoluminescence (PL) spectroscopy of individual QDs. PL spectroscopy of individual QDs using solid immersion lens (SIL) has a major advantage over conventional methods such as sample processing^{7,8} and near-field scanning microscopy:⁹ it optically accesses individual QDs while still maintaining relatively high efficiency of light collection, so that two-dimensional (2D) scan can be performed to find QDs of interest and that the interactions between neighboring QDs can be studied.

Two configurations of solid immersion technique have been widely discussed. One is using a hemispherical SIL (h-SIL) that improves the spatial resolution by a factor of n (refractive index of SIL), and is universal for any wavelength. The other is using a super-spherical SIL (s-SIL) in Weierstrass optics that further improves spatial resolution and collection angle by another factor of n ,¹⁰ but is designed only for one wavelength. Both have been applied to the study of QD spectroscopy and demonstrated higher spatial resolution and collection efficiency than those without using SIL.^{5,11,12} In the light of 2D scan, however, a stringent requirement is imposed on the overall and local flatness of the contacting surfaces between the SIL and the sample, because the intensity of QD PL is strongly dependent on the local variation of the gap for these two configurations. Here we apply to the QD PL spectroscopy a subsurface solid immersion technique that features a numerical aperture increasing

lens (NAIL).^{13–15} In this scheme, the contacting interface is moved away from the focal plane. The light waves of higher spatial frequency decay faster when they transit through the thin air gap that can possibly exist at the interface, usually in evanescent mode, and are attenuated more significantly than those of longer wavelengths. Here, the interface acts as a low-pass filter, causing a degradation in the entire image while keeping the overall fidelity. If the interface is at the image plane, nonuniformity will cause large fluctuations in the quality of the image, leading to artifacts. By using NAIL configuration, we diminish the influence of possible artifacts in the interface on the images obtained in a 2D scan. Meanwhile, our technique maintains the main advantages of generic SIM: high spatial resolution and high collection efficiency.

The experimental setup consists of a scanning confocal microscope and a NAIL-sample assembly. Figure 1(a) shows the layout of our experimental apparatus. The excitation light from a Ti:sapphire laser goes into the system through the side arm of the microscope. The sample is housed in a continuous helium flow cryostat with temperature as low as 4.2 K. The cryostat is mounted on an XYZ stage that features two nanomovers providing the scanning capability in X and Y directions with a precision of 10 nm. PL from the sample is collected by the same focusing objective (lens) in the microscope and then guided to the monochromator and detectors through a single-mode fiber in the top arm. Since the sample and NAIL move together with respect to the laser beam, the system will be slightly out of focus in a 2D scan when the sample and NAIL move away from the center. However, the typical scanning range of 20 μm is very small compared to the radius of NAIL (1610 μm). The system is in good focus and the spatial resolution is well maintained throughout the process of a 2D scan.

Figure 1(b) shows the detailed optics of the NAIL-sample assembly. The sample is self assembled InGaAs QDs sandwiched in GaAs barriers, with a uniform areal density of

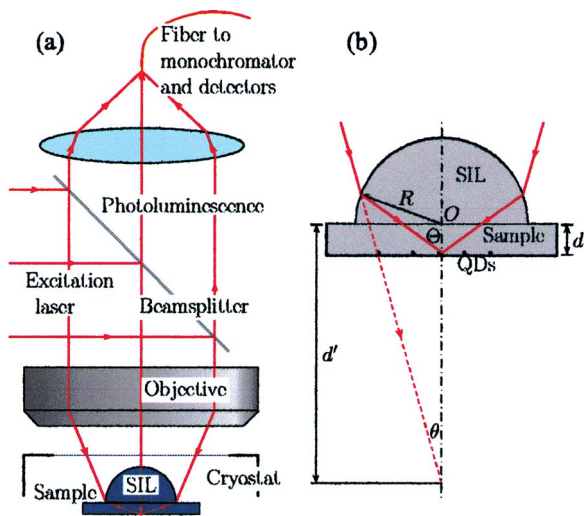


FIG. 1. (Color) The optical setup of the experiment. (a) Overview of optical layout. NAIL-sample assembly is placed inside a microscopic cryostat, which moves in X and Y directions during a 2D scan. (b) Optics of the NAIL-sample assembly. The hemispherical SIL is placed on the back side of the sample, whose thickness d satisfies $d=R/n$ for stigmatic imaging.

$\sim 10^8 \text{ cm}^{-2}$. It is placed upside down with a GaAs NAIL (here, it is an h-SIL) on top of it. The NAIL and the substrate of the sample are made of the same material. The bottom of the NAIL is in very good optical contact with the back surface of the sample so as to minimize the loss of PL intensity as well as the optical aberration at the interface. The thickness of the sample (d), the radius (R) and the refractive index (n) of the NAIL satisfy the relationship $d=R/n$, so that the NAIL-sample assembly operates in stigmatic mode. The magnification of this NAIL imaging system is approximately $M=d'/d$. This means that a step of Δx of the X - Y stage results in a step of $\Delta x/M$ in the subsurface focal plane. The stability of the system also benefits from this configuration, because any vibration of the physical setup is demagnified by a factor of M in the focal plane.

We define the full-width-at-half-maximum (FWHM) of the beam profile as the spatial resolution of this system, known as Houston criterion. It is close to $\lambda_0/(2 \cdot \text{NA})$, where λ_0 is the wavelength in vacuum and NA is the numerical aperture defined as $n \sin \theta$. For our optical configuration, we expect a resolution of $\sim 280 \text{ nm}$ in our experiment. To measure the real resolution in experiment, we scan over a point source and the FWHM of the point spread function (PSF) thus measured can be regarded as the actual spatial resolution of the optical system. If a source itself has a small width (D), then FWHM (W) of the PSF is the convolution of system resolution (R) and D : $W = \sqrt{R^2 + D^2}$. It is natural to consider a self-assembled InGaAs/GaAs QD as a point source, because its lateral size is usually less than $\sim 40 \text{ nm}$, which means $D < 40 \text{ nm}$. While R is known to be in the magnitude of 300 nm , W should be very close to R . Also considering the uncertainty in measurement, we can simply take the measured W as the actual spatial resolution of the system.

Figure 2 shows the measurement of the real spatial resolution of the system. Inset (a) is the 2D spatial distribution of the intensity of a sharp QD PL line, also known as the spectral image of a QD. Inset (b) is the linecut along X direction as marked by the arrow in inset (a). It yields a FWHM of 350 nm , which we regard as the real spatial resolution of our optical system. The discrepancy between the theoretical and

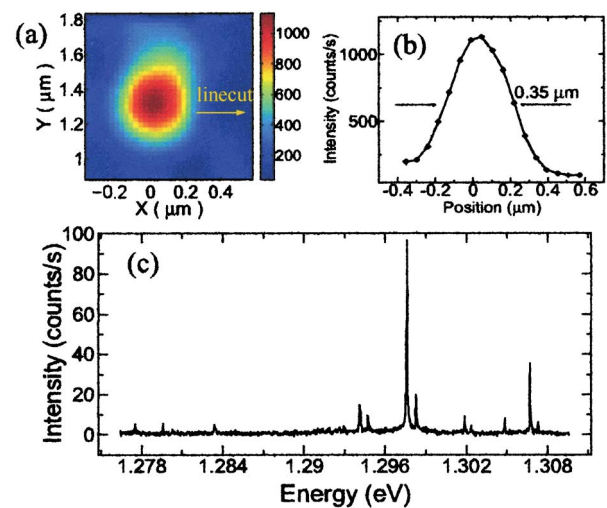


FIG. 2. (Color) Measurement of the spatial resolution of the optical system and its capability of resolving PL spectra of single QDs. Inset (a), 2D spatial distribution of the intensity of a sharp QD PL line. Inset (b), the linecut along X direction as marked by the arrow in inset (a). Inset (c), a typical PL spectrum of the QD taken with our microscope. Excitation laser energy: 1.476 eV . Temperature: 8 K .

measured values most likely arises from an air gap of $\lambda_0/10$ that may exist between the QD sample and the NAIL.¹⁴

With such a spatial resolution, our system is able to probe only a few QDs. Therefore the inhomogeneous line broadening is removed and the characteristic sharp lines of QD PL should be observed. Figure 2(c) shows a typical spectrum of QD PL taken at 8 K with this system. We can see that only a few sharp lines are prominent over a low and flat background, producing a spectroscopic evidence that the spatial resolution achieved by our SIM is suitable for optical studies of individual QDs.

To demonstrate the high collection efficiency of our system, we compare the peak PL intensities of the same QD sample taken with and without NAIL. For the former configuration, the objective as in Fig. 1(a) is replaced by an achromatic lens optimized at near infrared with $\text{NA}=0.12$, namely $\sin \theta=0.12$ where θ is shown in Fig. 2(b). For the latter configuration, a Zeiss $40\times$ objective is used, with $\text{NA}=0.6$. All other elements of the experimental setup are the same for both configurations. Because the PL measurements of these two configurations are performed at different time under different excitation power, a few notes must be heeded in order to make this comparison of collection efficiency meaningful. First, this is a uniform sample. Statistically, intensities of PL from QDs in different areas of the sample are in the same order of magnitude. Second, only saturated PL intensities are comparable. This is because the saturated PL intensity of a QD is independent of excitation power. Otherwise, one could always increase the excitation power to see higher PL intensity, rendering the comparison of system throughput questionable. Third, statistical results of multiple QDs should be used to counteract the adverse effect caused the inhomogeneity of optical properties of individual QDs.

We scan an area on the sample where more than 10 QDs are located. A PL spectrum is recorded at each grid point of the 2D scan. The excitation power is set at a level such that the QD PL is saturated. We then plot the spectral images of the brightest PL lines. Each spectral image indicates the spa-

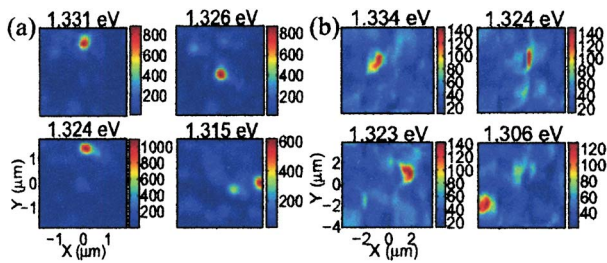


FIG. 3. (Color) Representative spectral images of brightest QDs with saturated PL intensities. The unit of the color scale bars is counts/second. (a) measured with NAIL microscope; (b) with conventional high NA objective, without NAIL.

tial position of a QD emitting that PL line. Thus we map out the QDs in the scanned area and find out the saturated PL intensities of these brightest QDs. Figure 3(a) shows the spectral images of the five PL lines measured with NAIL while Fig. 3(b) are those measured without NAIL. The backgrounds are seemingly different in these two insets because the intensity scales are different. PL in (a) has a higher peak-to-background ratio that suppresses the image noise. The images in (a) also appear more smooth than those in (b). This is because the vibration noise is reduced by a factor of M , the magnification of this surface imaging system. Some spectral images have the same or very similar spatial pattern, such as the first images of the two rows in Fig. 3(a). This indicates that those PL lines originate from different emission states of the same QD, thus provides a useful method to identify PL lines from different quantum states of the same QD. In this case, we take the spectral image of the strongest intensity to represent that QD in statistical intensity comparison of multiple QDs.

Judging by their spatial patterns, we locate the brightest thirteen QDs for each measurement configuration. Their peak intensities are shown in the scatter graph of Fig. 4. Each marker represent a QD. The red ones are imaged through NAIL, with the mean value of the intensity being 830 counts per second (cps), and standard deviation 137 cps. The blue ones are imaged with the conventional microscope without NAIL, with the mean value of 138 cps and standard deviation of 9 cps. For each measurement configuration, the variation of intensity among these QDs is 16% and 7%, respectively. This indicates that the sample is relatively uni-

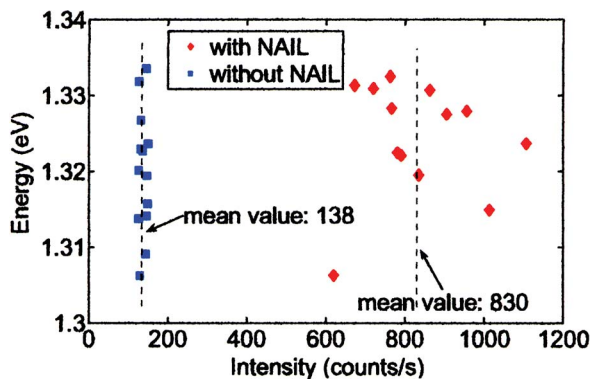


FIG. 4. (Color) Peak intensities of the thirteen brightest QDs for each configuration. Intensities are measured by a liquid nitrogen cooled Si CCD camera. The red markers represent the QDs imaged with NAIL while the blue ones without. The vertical dash lines indicate the mean values of intensity.

form and that the comparison of collection efficiency on a statistical basis should be solid and reliable. Therefore, comparing the mean values of peak intensities, we find that PL measurement using NAIL technique sees an improvement of collection efficiency by a factor of six over that using conventional high NA objective.

Now we discuss the origins of this improvement. For a specific light emitter, the ability to collect its emission in far field is usually determined by the solid angle and the transmission of collection optics. In terms of solid angle, the optical configuration of our NAIL system doesn't have the advantage over the conventional high NA objective, because the solid angle, though improved by a factor of n through the Weierstrass optics, is only 0.42, still less than the NA of the Zeiss objective, 0.6.

Then the improvement of collection efficiency must come from the increase of transmission. It is known that radiation pattern of a dipole on or near a flat surface of dielectric medium is stronger in the medium of higher refractive index.¹⁶ In our case, the QDs emit more light into the substrate of sample and NAIL than into the air. Then the PL transmits through the sample-air interface or the NAIL-sample assembly to reach the collection objective. Combining the calculation by Koyama *et al.*³ and Ippolito *et al.*,¹⁴ we estimate the improvement should be ~ 5 . This is consistent with our experimental result.

In summary, we applied the NAIL technique to the microscopic PL spectroscopy of individual QDs, whose main benefits are improved resolution, collection efficiency, and uniformity of transmission across the gap throughout the field of view. We achieved a spatial resolution of ~ 350 nm that is high enough to resolve the spectroscopic features of single QDs. We also demonstrated that the collection efficiency of the system with NAIL is 6 times better than that of a conventional confocal microscope with a high NA objective.

This work was supported by Air Force Office of Scientific Research under Grant No. MURI F-49620-03-1-0379 and by NSF under Grant No. NIRT ECS-0210752.

¹S. M. Mansfield and G. S. Kino, Appl. Phys. Lett. **57**, 2615 (1990).

²M. Yoshita, T. Sasaki, M. Baba, and H. Akiyama, Appl. Phys. Lett. **73**, 635 (1998).

³K. Koyama, M. Yoshita, M. Baba, T. Suemoto, and H. Akiyama, Appl. Phys. Lett. **75**, 1667 (1999).

⁴B. B. Goldberg, S. B. Ippolito, L. Novotny, Z. Liu, and M. S. Ünlü, IEEE J. Sel. Top. Quantum Electron. **8**, 1051 (2002).

⁵S. Moehl, H. Zhao, B. D. Don, S. Wachter, and H. Kalt, J. Appl. Phys. **93**, 6265 (2003).

⁶V. Zwiller and G. Björk, J. Appl. Phys. **92**, 660 (2002).

⁷D. Gammon, E. S. Snow, B. V. Shanabrook, D. S. Katzer, and D. Park, Phys. Rev. Lett. **76**, 3005 (1996).

⁸K. Hinzer, P. Hawrylak, S. Fafard, M. Bayer, O. Stern, A. Gorbunov, and A. Forchel, Phys. Rev. B **63**, 75314 (2001).

⁹H. D. Robinson and B. B. Goldberg, Phys. Rev. B **61**, R5086 (2000).

¹⁰M. Born and E. Wolf, *Principles of Optics*, 7th ed. (Cambridge University Press, Cambridge, U.K., 1999), p. 159.

¹¹V. Zwiller, H. Blom, and P. Jonsson, Appl. Phys. Lett. **78**, 2476 (2001).

¹²Q. Wu and R. Grober, Phys. Rev. Lett. **83**, 2652 (1999).

¹³S. B. Ippolito, B. B. Goldberg, and M. S. Ünlü, Appl. Phys. Lett. **78**, 4071 (2001).

¹⁴S. B. Ippolito, B. B. Goldberg, and M. S. Ünlü, J. Appl. Phys. **97**, 053105 (2005).

¹⁵S. B. Ippolito, S. A. Thorne, M. G. Eraslan, B. B. Goldberg, M. S. Ünlü, and Y. Leblebici, Appl. Phys. Lett. **84**, 4529 (2004).

¹⁶K. H. Drexhage, Prog. Opt. **12**, 163 (1974).